Experimental Study of the Micro and Macro Scale Compression Behavior of a Sand Immersed in a Viscous Liquid

Wang Wanying[a], Chen Degao[a], Matthew R. Coop[b], Yuan Bingxiang[a]

[a] Guangdong University of Technology

[b] University College London

ABSTRACT

Pore fluids with different viscosities can exist in soils. While the effects of pore fluids have been investigated at the macro-scale, little is known about how they might affect the micromechanics. A novel apparatus allowing a single particle to be crushed while immersed in a liquid was built here. With the help of a high-speed microscope camera, the crushing processes of single silica sand particles immersed in glycerin were captured and the breakage modes were clarified. The immersion in glycerin leads to stronger particles with higher strains at failure compared with immersion in water or exposure to air. Moreover, the results of CRS tests revealed that saturation in glycerin made the sample significantly stiffer in compression as a result of less particle breakage compared with that in water or under dry conditions. The lower particle breakage at the macro-scale appeared to correspond to the higher strengths measured at the micro-scale.

Word count: 1990 words for main body of the text.

Introduction

Typically clastic materials such as sands and rockfills show greater particle damage under loading when immersed in water and this apparent strength loss has been attributed to various possible mechanisms within fissures in the particles such as intra-particle suction, the stress corrosion effect of water or the variation of surface energy caused by the water adsorption and mineral dilution (Coop & Lee, 1995; Michalske & Freiman, 1982; Oldecop & Alonso, 2001). Besides water, other kinds of liquid could also fill in the voids in natural sands, such as oil in reservoir sands or oil contamination of soils due to spillage during drilling or transportation in the offshore oil industry. The presence of oil could, for example, affect the geotechnical properties of seabed soils, which could compromise the stability of an offshore platform (Ajagbe et al., 2012; Khosravi et al., 2013). The presence of a non-water fluid can change the internal friction angle and the capacity of soils, often decreasing it, while increasing the volumetric strains leading to higher compressibilities and larger settlements (Evgin & Das, 1992; Shin et al., 2002; Nasr, 2009).

Meegoda & Rajapakse (1994) indicated that the variation of the viscosity of the pore fluid contributed to the variation of the compression index as well as the liquid limit of clay soils. Ratnaweera & Meegoda (2006) found a reduction of shear strength that was attributed to the change of the mineral-pore fluid interactions resulting in an expansion of the electrical double layer thickness according to the electrical double layer theory. Fine et al. (1997) investigated how the increase of the viscosity of pore fluids changed the permeability of soils. However, how a viscous liquid affects the single particle breakage behaviour under loading needs to be addressed.

In this study, a novel apparatus was used to investigate the mechanical response and the breakage performance of a single silica sand particle immersed in glycerine. The results were compared with those in air or water to study the effect of viscosity of pore fluids on the breakage modes as well as the mechanical behaviour of a single particle under uniaxial compression. Finally, oedometer tests with a constant rate of strain were conducted on silica sands saturated in glycerine, water and dry, respectively, to study the relationships between the macro and micro geotechnical properties of silica sands under different loading conditions.

Apparatus and materials

Leighton Buzzard Sand (LBS) (a silica sand) with a fraction of 1.18-2.36mm was tested in this study. Glycerine is a colourless, odourless and viscous liquid, which is largely inert and so would not react with silica physically or chemically. In temperature of 20℃, the viscosity of glycerine is about 1500×10^{-3}Pa s, which is almost 1500 times of that for water at this temperature.

Figure 1 shows that the custom-built apparatus system used in this research. Compression was applied at 0.1mm/min and the force acting on the single particle was recorded by a load cell with a capacity of 1000N and a resolution of 0.1N. The vertical deformation of the particle was measured by a high-resolution LVDT with a linear range of 8mm and a resolution of 1μm. A high-speed camera with a frame rate of 750 f/s is necessary to capture the extremely rapid breakage of silica sand grains. In this study, a single particle was designed to be crushed when immersed in glycerine. Therefore, a liquid container and a matching loading platen were built (Figure 2). A

transparent glass box was located on the lower mount to enable the particle breakage process observed.

To investigate the relationship between the macro and micro mechanical properties of silica sands under different loading conditions (in air and saturated in glycerine or water), constant rate strain oedometer tests (CRS) were also conducted on LBS in air and saturated in glycerine or water. The specimen with a diameter of 61.8mm and initial height about 20mm was compressed between two pieces of porous stone. The maximum stress applied was around 33MPa with a low constant loading rate of 0.001mm/s to ensure a good drainage.

Crushing modes of single sand particles immersed in glycerine

Figure 3(a) illustrates a typical relationship between the normal force and vertical displacement, followed by a corresponding a series of particle images for the same test in Figure 3(b). To understand better the particle splitting process, sketches are shown in Figure 4. The normal force increased approximately linearly with the vertical displacement until a maximum value and then dropped to zero suddenly. At point 2 of the force-displacement curve, a shadow implying a crack initiation occurred at the upper contact surface of the particle (Figure 3b-2). It is noted that the crack initiation here has little effect on the mechanical response of the single particle and it can be seen from Figure 3(a) that the force-displacement response even stiffens after this point. At point 3, the shadow enlarges towards the central part of the particle, followed by the appearance of a bright region in the middle. Then the particle split into two main parts without creating many fragments, which was called the “splitting

mode" by Wang & Coop (2016). The speed of the crack propagation was extremely high and takes about 0.01s.

Another typical crushing process, in which the crack initiates in the central section of the particle instead of a contact surface is illustrated in Figure 5 and 6. In this case, an initial softer mechanical response under small load could be observed, which could be attributed to the adjustment of the particle position between the platens, possibly promoted by the lubrication of the glycerine. After the point 1, the force-displacement curve stiffens dramatically, during which a shadow occurs in the upper right region inside the particle, which then propagates gradually (Figure 5b2-3). At the first peak (point 4) of the curve, it could be observed that the meridional crack propagates rapidly, within 0.01 second, leading to the particle splitting into two pieces of different sizes. After the first drop of the force, strain hardening could be observed with the particle carrying even more load. It is noted that only a splitting mode was found for glycerine immersed particles. This reveals the difference of breakage processes between particles immersed in glycerine and those in water or under dry conditions. In the latter two testing conditions explosive modes were also found, where a single particle blasts into a large number of fragments catastrophically and instantaneously (Wang & Coop, 2016).

Effect of the pore fluid viscosity on the micro and macro mechanical behaviour

The compression strengths of single LBS particles in different loading conditions were analysed by means of Weibull statistics as shown in Figure 7(a). The characteristic strengths σ_0 of single LBS particles, i.e., the strength for which 37% of the particles have a strength higher than or equal to this value, are 45.4MPa, 43.4MPa and 74.1MPa compressed in air, water and glycerine, respectively. The results show

that the compressive strength of single particles immersed in glycerine is much higher than that in dry and water conditions. The Weibull modulus m, which is used to describe the uniformity of the strengths, is plotted in Figure 7(b). The m for LBS in dry conditions is around 1.5 for $\sigma_0 \leq \sigma$ and around 3 for $\sigma_0 > \sigma$, while for immersion in water, m is 2 for $\sigma_0 \leq \sigma$ and around 4 for $\sigma_0 > \sigma$. This illustrates that the strengths are more uniform for water immersed which can also be seen in Figure 7(a), in which the inclination of the Weibull statistic curve for dry conditions is a bit lower. When the particles are immersed in glycerine, the value of m is around 4 for $\sigma_0 \leq \sigma$ and 5 for $\sigma_0 > \sigma$, which indicates that the strength distribution is narrower than for immersion in water or air.

The average and standard deviation values of peak stress as well as nominal strains in different loading conditions (in air and saturated in glycerine or water) are plotted in Figure 8. The mean values of peak stress and nominal strains for single particles immersed in water (41.6 MPa and 0.016, respectively) are lower than that in dry condition (44.7 MPa and 0.022, respectively). However, the mean values of the peak stress and the nominal strains of single particles in glycerine are 65.4MPa and 0.050, respectively, which are much greater than that for the other two loading conditions. Since glycerine is inert for quartz particles it can be proposed that it is the viscosity of the glycerine that causes the particles to be stronger. Cavarretta et al. (2011) found that glycerine has a lubricating effect that may lead to a reduction of friction between the loading platen and the particle. This would also affect the normal contact stresses at the particle contacts, which, in turn, influence the stress distribution inside single particles. Coop & Lee (1995) suggested that intra-particle suctions could influence particle strengths and another possible mechanism that might explain the different

strengths is that the greater viscosity of the glycerine might allow greater suctions to exist within any natural fissures in the particles. Under the atmospheric pressure, glycerine is more likely to "coat" around the surface of particles instead of entering the internal fissures. A third possible reason is that the different chemical properties of glycerine and water might affect the stress corrosion at the tip of cracks developing inside the particles. However, it is not possible to determine which of these mechanisms is responsible.

To investigate the relationship between the micro and macro mechanical properties of LBS in different loading conditions, a series of constant strain rate oedometer tests were conducted. The e-lgσ curves of LBS in air, saturated in water and glycerine are plotted in Figure 9. The initial void ratio of the specimen for each test is the same, i.e., 0.652 and the maximum stress experienced by the specimen for each test was 33.33 MPa. The curves indicate that the yield pressures of the samples under different loading conditions are similar, i.e., 6.66MPa. However, presence of glycerine leads to a lower compressibility of the sand sample while water gives slightly higher compressibility. The particle size distributions (PSD) measured by sieving after the tests are shown in Figure 10 along with the PSD before testing. Under the maximum stress of 33.3 MPa, there was significant breakage of the LBS particles for all three conditions, but it can be observed that there is slightly less breakage with glycerine, corresponding to the higher location of the NCL while there is slightly more breakage in water, corresponding to the lower location of the NCL. This is consistent with the strengths measured in the single particle tests, although it is perhaps surprising that quite large differences of particle strength for single particles in Figure 8(a) only result in quite small changes to the grading of the whole sample. It is interesting that

the lower inter-particle friction that would occur in glycerine (Cavarretta et al., 2011) might tend to cause greater compressibility, but this seems to be less important than the effect of the reduced breakage.

Conclusion

The mechanical response and breakage behaviour of single silica sand particles immersed in a viscous liquid, i.e., glycerine, were investigated in both microscopic and macroscopic scales. In the single particle compression tests, only a splitting mode was found, while an explosive mode could also be observed for particles compressed in air and immersed in water (Wang & Coop. 2016). Although the cracks initiated and propagated prior to the final failure, they had little effect on the force-displacement curve before the peak. Particles immersed in glycerine tend to be stronger with a larger nominal strain at failure, compared to those compressed in air and in water. At the macro-scale, CRS tests showed that LBS specimens saturated in glycerine tend to have a lower compressibility and less particle breakage compared with those in air or immersed in water, which is consistent with the micro-mechanical tests. These differences of particle strength at both scales could possibly be attributed to one of three mechanisms, i) differences of stress corrosion within micro-fissures at failure, ii) higher intra-particle suctions within natural fissures in the particles because of the higher viscosity of the glycerine, or iii) lubrication effects at the particle contacts changing the contact stress regime.

Acknowledgements

The study was financially supported by National Natural Science Foundation of China (Grant No. 51809050), Guangdong Basic and Applied Basic Research Foundation

(Grant No. 2020A1515010811) and Guangzhou Basic and Applied Basic Research Project (Grant No. 202201010391).

References

Ajagbe, W.O., Omokehinde, O.S., Alade, G.A., Agbede, O.A., Effect of Crude Oil Impacted Sand on compressive strength of concrete, Constr. Build. Mater. 26 (2012) 9–12. https://doi.org/10.1016/j.conbuildmat.2011.06.028.

Cavarretta, I., The influence of particle characteristics on the engineering behaviour of granular materials, PhD thesis, Imperial College London, 2009.

Cavarretta, I., Rocchi, I., Coop, M.R., A new interparticle friction apparatus for granular materials, Can. Geotech. J. 48 (2011) 1829–1840. https://doi.org/10.1139/t11-077.

Coop, M.R., Lee, I.K., The influence of pore water on themechanics of granular soils, in: Proc. XIth Eur. Reg. Conf. SMFE, Copenhagen, Denmark, 1995: pp. 63–73.

Evgin, E., Das, B.M., Mechanical behavior of an oil contaminated sand, in: Mediterr. Conf., Balkema, Rotterdam, The Netherlands, 1992: pp. 101–108.

Khosravi, E., Ghasemzadeh, H., Sabour, M.R., Yazdani, H., Geotechnical properties of gas oil-contaminated kaolinite, Eng. Geol. 166 (2013) 11–16. https://doi.org/10.1016/j.enggeo.2013.08.004.

203 Meegoda, N.J., Rajapakse, R.A, Short-term and long-term permeabilities of
204 contaminated clays, Int. J. Rock Mech. Min. Sci. Geomech. Abstr. 31 (1994)
205 139. https://doi.org/10.1016/0148-9062(94)90610-6.
206 Michalske, T.A., Freiman, S.W., A molecular interpretation of stress corrosion in
207 silica, Nature. 295 (1982) 511–512. https://doi.org/10.1038/295511a0.
208 Nasr, A.M.A., Experimental and Theoretical Studies for the Behavior of Strip Footing
209 on Oil-Contaminated Sand, J. Geotech. Geoenvironmental Eng. 135 (2009)
210 1814–1822. https://doi.org/10.1061/(ASCE)GT.1943-5606.0000165.
211 Oldecop, L.A., Alonso, E.E., A model for rockfill compressibility, Géotechnique. 51
212 (2001) 127–139. https://doi.org/10.1680/geot.2001.51.2.127.
213 Oldecop, L.A., Alonso, E.E.,Suction effects on rockfill compressibility, Géotechnique.
214 53 (2003) 289–292. https://doi.org/10.1680/geot.2003.53.2.289.
215 Ratnaweera, P., Meegoda, J.N., Shear strength and stress-strain behavior of
216 contaminated soils, Geotech. Test. J. 29 (2006) 133–140.
217 https://doi.org/10.1520/gtj12686.
218 P. Fine, E.R. Graber, B. Yaron, Soil interactions with petroleum hydrocarbons:
219 Abiotic processes, Soil Technol. 10 (1997) 133–153.
220 https://doi.org/10.1016/S0933-3630(96)00088-8.
221 Shin, E., Omar, M., Tahmaz, A., Das, B., C.B.T.-4th I.C. on E.G. Atalar, Shear
222 Strength and Hydraulic Conductivity of Oil-Contaminated Sand, in: 2002.

223 Wang W., Coop, M.R., An investigation of breakage behaviour of single sand
224 particles using a high-speed microscope camera, Géotechnique. 66 (2016) 984–
225 998. https://doi.org/10.1680/jgeot.15.P.247.
226 Weibull, W., Discussion: A statistical distribution function of wide applicability, J.
227 Appl. Mech. 19 (1952) 233–234.
228
229
230
231
232
233
234
235
236
237
238
239
240
241
242

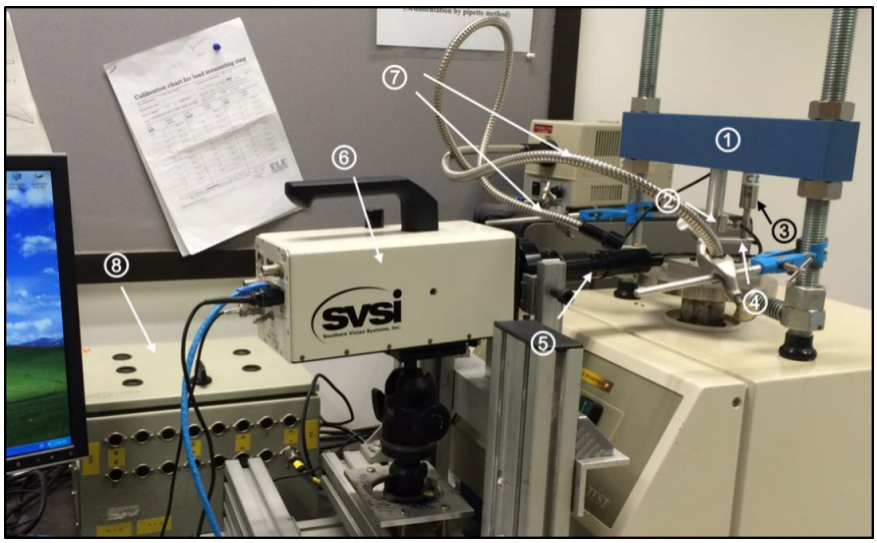

Figure 1 Apparatus of uniaxial compression test on single particle immersed in glycerine: ① Loading frame; ② Load cell; ③ LVDT; ④ Loading mounts; ⑤ Microscope lens; ⑥ High-speed camera; ⑦ High-intensity focused light; ⑧ Data logger.

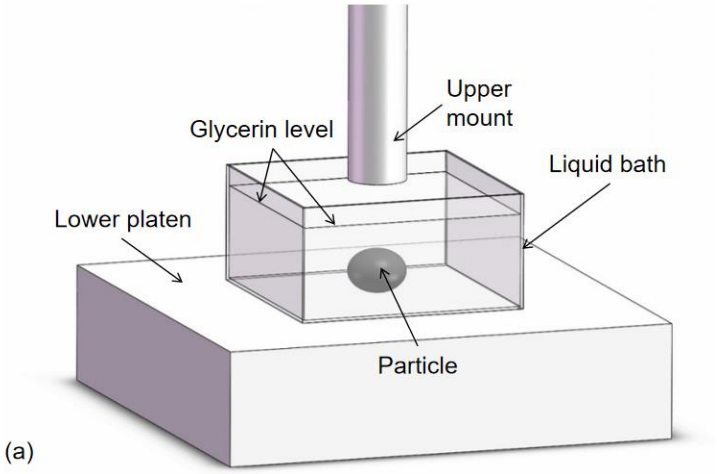

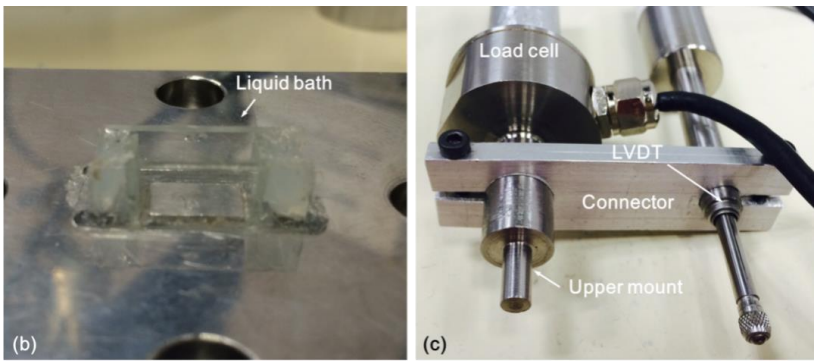

Figure 2 Details of the load application: (a) schematic diagram of loading platen and liquid bath; (b) details of liquid bath; (c) The details of the upper loading mount, load cell and LVDT.

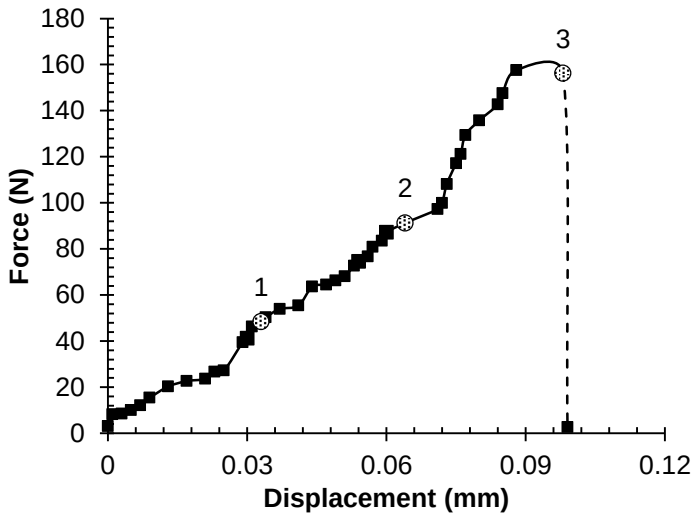

(i)

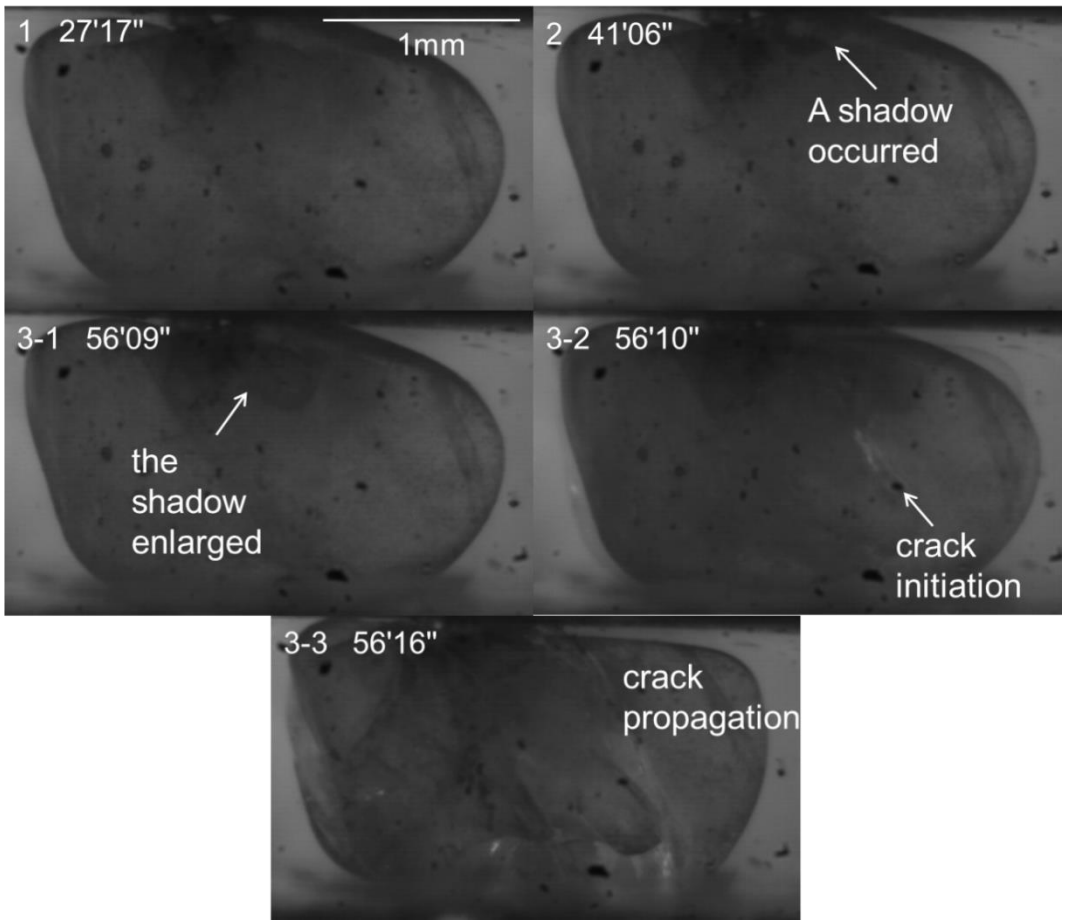

(ii)

Figure 3 A typical crushing process with crack initiation at edge of a single particle (1.18~2.36mm) immersed in glycerine: (i) force-displacement curve; (ii) image series of the breakage behaviour.

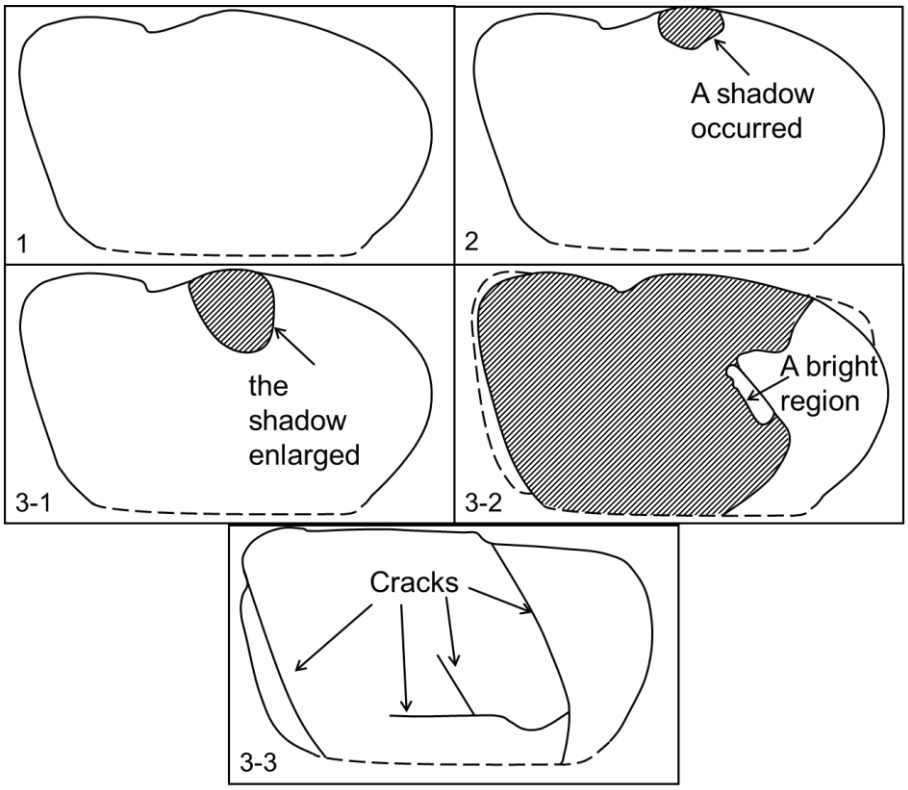

257

258 Figure 4. Sketch of the crack initiation at edge of the single particle, corresponding to Figure
259 3(ii).

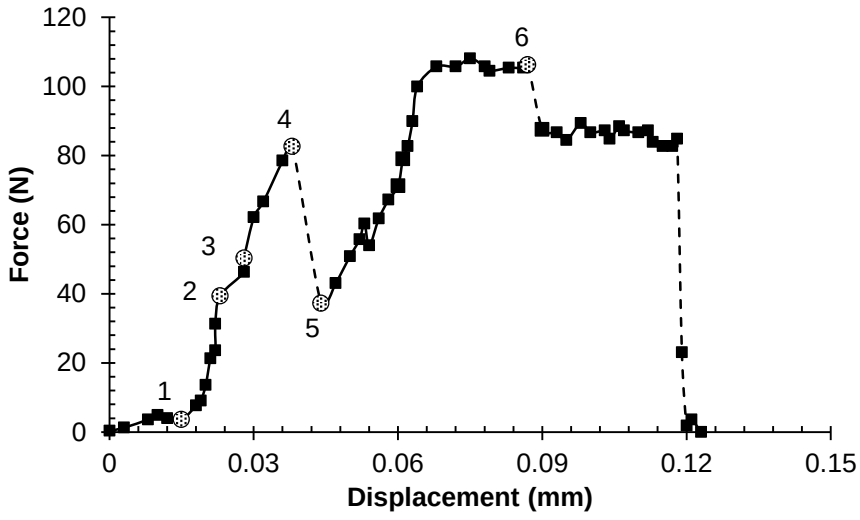

260 (i)

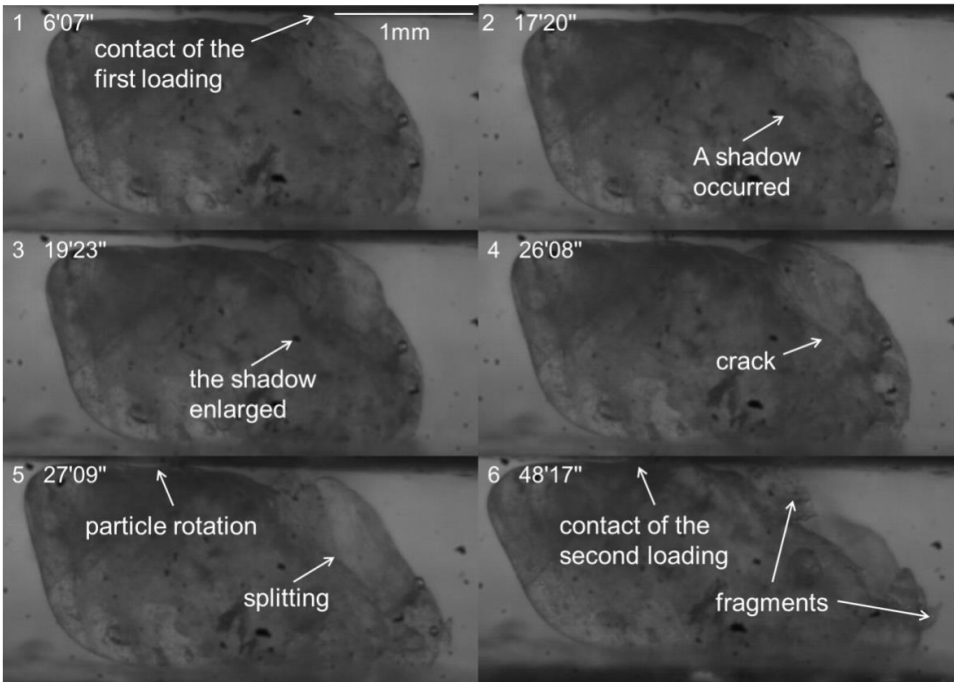

(ii)

Figure 5 A typical crushing process with crack initiation in central section of a single particle (1.18~2.36mm) immersed in glycerine: (i) force-displacement curve; (ii) image series of the breakage behaviour.

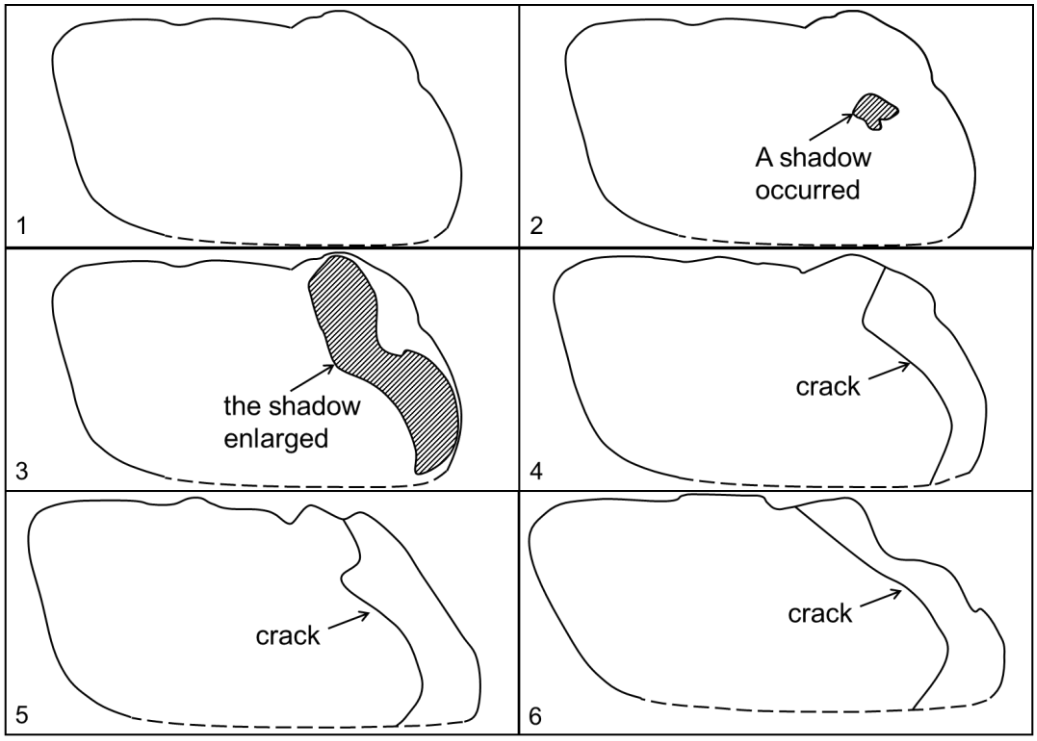

Figure 6 Sketches of the crack initiation in the central section of a single particle, corresponding to Figure 5(ii).

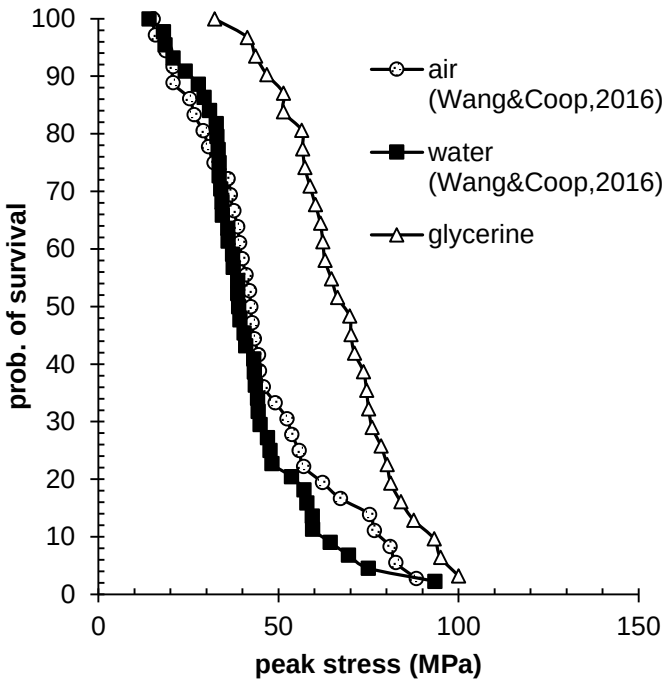

(a)

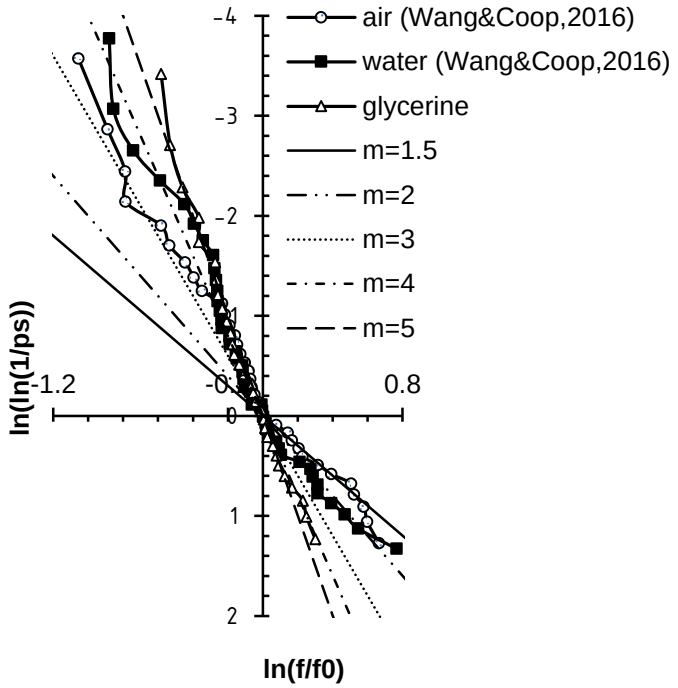

(b)

Figure 7(a) Comparison of strengths of single LBS particles under different loading conditions (b) m-modulus (data for air and water immersed from Wang and Coop, 2016).

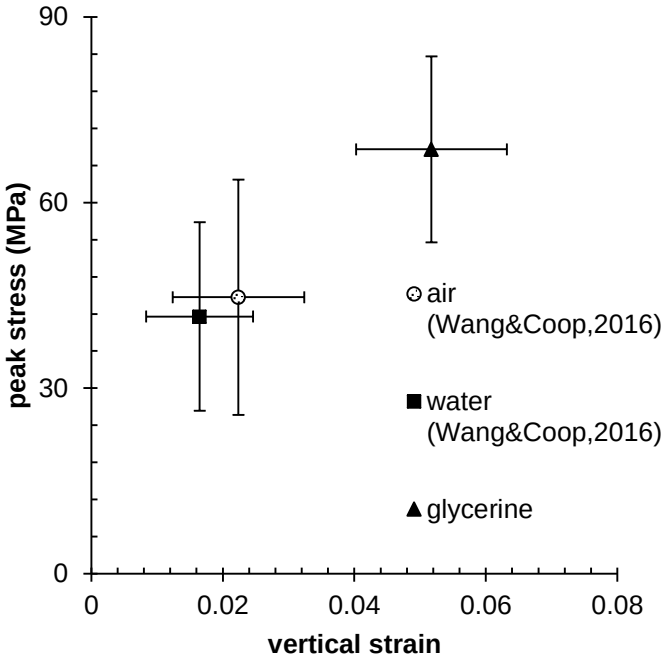

Figure 8 Comparison of strengths and nominal strains of single particles compressed in different loading conditions in terms of mean value and standard deviation (data for air and water immersed from Wang and Coop, 2016).

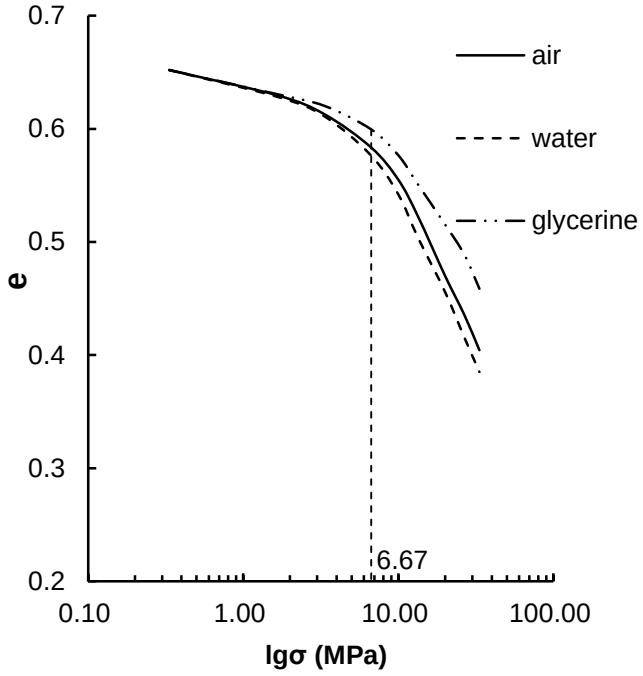

Figure 9 Constant rate of strain oedometer (CRS) tests LBS (1.18~2.36mm) in air, water and glycerine.

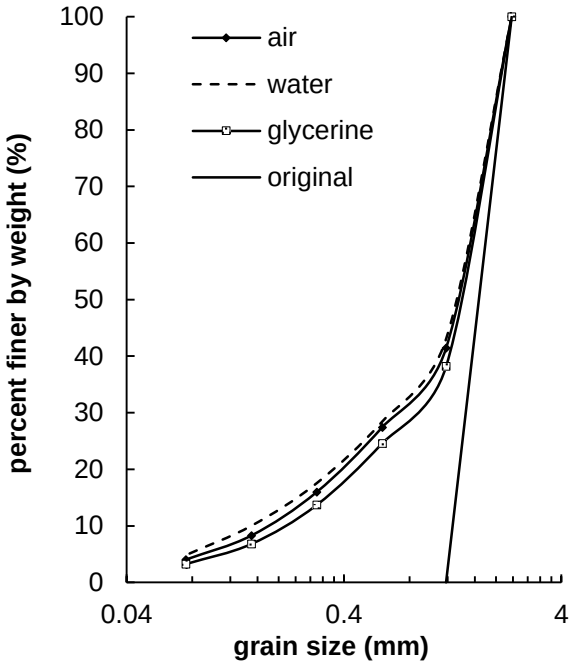

Figure 10 Particle size distribution curves of LBS samples (1.18-2.36mm) under different loading conditions before and after tests corresponding to Figure 10 with a maximum load of 33.3 MPa.